Original Article

Optical navigation robot-assisted puncture system for accurate lung nodule biopsy: an animal study

Jing Li[1,2#], Liyilei Su[3#], Jun Liu[4], Qian Peng[2], Rongde Xu[5], Wei Cui[5], Yi Deng[1], Weiguo Xie[4], Bingding Huang[3]^, Jingjing Chen[2]

[1]Department of Pulmonary and Critical Care Medicine, The First People's Hospital of Yunnan Province, The Affiliated Hospital of Kunming University of Science and Technology, Kunming, China; [2]Department of Pulmonary and Critical Care Medicine, Guangdong Provincial People's Hospital (Guangdong Academy of Medical Sciences), Southern Medical University, Guangzhou, China; [3]College of Big Data and Internet, Shenzhen Technology University, Shenzhen, China; [4]Wuerzburg Dynamics Inc., Shenzhen, China; [5]Department of Interventional Radiology, Guangdong Provincial People's Hospital (Guangdong Academy of Medical Sciences), Southern Medical University, Guangzhou, China

Contributions: (I) Conception and design: J Li, W Xie, B Huang; (II) Administrative support: W Xie, B Huang, J Chen; (III) Provision of study materials or patients: J Li, Y Deng, J Chen; (IV) Collection and assembly of data: J Liu, Q Peng, R Xu, W Cui; (V) Data analysis and interpretation: L Su, J Liu, J Chen; (VI) Manuscript writing: All authors; (VII) Final approval of manuscript: All authors.

[#]These authors contributed equally to this work.

Correspondence to: Jingjing Chen, MM. Department of Pulmonary and Critical Care Medicine, Guangdong Provincial People's Hospital (Guangdong Academy of Medical Sciences), Southern Medical University, 106 Zhongshan 2nd Road, Guangzhou 510080, China. Email: chenjingjing0217@gdph.org.cn; Bingding Huang, PhD. College of Big Data and Internet, Shenzhen Technology University, 3002 Lantian Road, Shenzhen 518118, China. Email: huangbingding@sztu.edu.cn.

Background: As lung cancer is one of the most significant factors seriously endangering human health, a robot-assisted puncture system with high accuracy and safety is urgently needed. The purpose of this investigation was to compare the safety and effectiveness of such a robot-assisted system to the conventional computed tomography (CT)-guided manual method for percutaneous lung biopsies (PLBs) in pigs.

Methods: An optical navigation robot-assisted puncture system was developed and compared to the traditional CT-guided PLB using simulated lesions in experimental animals. A total of 30 pulmonary nodules were successfully created in 5 pigs (Wuzhishan pig, 1 male and 4 females). Of these, 15 were punctured by the optical navigation robot-assisted puncture system (robotic group), and 15 were manually punctured under CT guidance (manual group). The biopsy success rate, operation time, first needle tip-target point deviation, and needle adjustment times were compared between groups. Postoperative CT scans were performed to identify complications.

Results: The single puncture success rate was higher in the robotic group (13/15; 86.7%) than in the manual group (8/15; 53.3%). The first puncture was closer to the target lesion (1.8±1.7 mm), and the operation time was shorter (7.1±3.7 minutes) in the robotic group than in the manual group (4.4±2.8 mm and 12.9±7.6 minutes, respectively). The angle deviation was smaller in the robotic group (3.26°±2.48°) than in the manual group (7.71°±3.86°). The robotic group displayed significant advantages ($P<0.05$). The primary complication in both groups was slight bleeding, with an incidence of 26.7% in the robotic group and 40.0% in the manual group. There was 1 case of pneumothorax in the manual group, and there were no deaths due to complications in either group.

^ ORCID: 0000-0002-4748-2882.

Conclusions: An optical navigation robot-assisted system for PLBs guided by CT images was developed and demonstrated. The experimental results indicate that the proposed system is accurate, efficient, and safe in pigs.

Keywords: Percutaneous lung biopsy (PLB); computed tomography (CT); computed tomography-guided biopsy (CT-guided biopsy); optical navigation robot-assisted puncture system

Submitted Apr 26, 2023. Accepted for publication Sep 06, 2023. Published online Oct 10, 2023.
doi: 10.21037/qims-23-576
View this article at: https://dx.doi.org/10.21037/qims-23-576

Introduction

Lung cancer is one of the greatest factors seriously endangering human health. The cancer statistics of the American Cancer Society for 2022 showed that morbidity and mortality due to lung cancer ranked second and first, respectively, in both men and women (1). Delayed diagnosis is a contributing factor to lung cancer's high mortality. Therefore, the detection and diagnosis of early-stage lung cancer are of great importance. Under the recommendations in lung cancer screening guidelines of many authoritative medical organizations in Europe and the United States (2), low-dose computed tomography (CT) has been widely used in clinical practice. Therefore, the detection rate of small and ground glass nodules (GGNs) has greatly improved, making early lung cancer diagnosis and treatment possible. However, the management of peripheral small pulmonary nodules remains a diagnostic challenge.

The 3 most common methods for diagnosing peripheral pulmonary nodules are bronchoscopy, transthoracic puncture, and surgery. The diagnostic yield for bronchoscopy alone remains as low as 33% (3). Even with new technologies such as electromagnetic navigation (4), virtual bronchoscopic navigation (5), and radial endobronchial ultrasound (6), the diagnostic yield is around 70% (7). Surgery is more invasive, costly, and complex than the other 2 methods. Transthoracic lung biopsy has unique advantages, especially for peripheral nodules. CT-guided transthoracic lung biopsy is widely accepted (8-10). However, the incidence of complications is high, pneumothorax and bleeding are 15% and 1%, respectively, and 17.8% of patients with hemorrhage require a blood transfusion (11). The operator's proficiency primarily determines the biopsy success rate. In addition, multiple CT scans may be required to adjust the needle during the procedure, and the patients are at higher risk of repeated radiation exposure and puncture. A robot-assisted system with a high diagnostic yield in the periphery without increased complications and radiation exposure is urgently needed (12).

A novel optical navigation robot-assisted puncture system has been developed to allow physicians to perform image-guided transthoracic needle aspiration. This system includes a unique optical navigation system that assists physicians in performing needle biopsies of lung nodules. This system aims to provide a much-needed intervention allowing physicians to use a robot-assisted puncture system for accurate biopsies with limited complications. As the pig lung and the human lung have very similar lobar and bronchial structures, and the pig lung is comparable in size to the human lung, it is a good animal model that can mimic the human lung. Therefore, we chose the pig lung as the animal model to validate our robot-assisted puncture system, which can effectively simulate real clinical scenarios. The objective of this animal study was to evaluate the robotic system's feasibility, safety, and accuracy in animal experiments and compare it with the conventional CT-guided manual method for transthoracic lung biopsy. We present this article in accordance with the ARRIVE reporting checklist (available at https://qims.amegroups.com/article/view/10.21037/qims-23-576/rc).

Methods

Experimental animals

A protocol was prepared before the study without registration. This animal study used 5 isolated healthy experimental Wuzhishan pigs (13,14) (1 male and 4 females, purchased from the Kangtai Forage Co. Ltd., Yangjiang, Guangdong, China; license No. SCXK(YUE)2020-0049) aged 6–9 months and weighing 25–40 kg. The experimental protocol was approved by the Ethics Committee of Guangdong Provincial People's Hospital (No. KV-Q-2022-214-01). This study was performed in the animal laboratory

at Silver Snake (Guangzhou) Medical Co. Ltd. Guangzhou, according to institutional guidelines for the care and use of animals.

Pigs selected for animal experiments were in good shape with no obvious trauma that would prevent optical markers from being attached to the body surface, able to breathe normally on their own, had no respiratory disease, and had a symmetrical thorax with clear texture and no large abnormal density areas in both lungs after CT examination. The selected female pigs were not in gestation or lactation. During the experiment, pigs were excluded if they had uncorrectable coagulation disorders or significant abnormalities in coagulation, other diseases such as pulmonary blisters or cysts in the proposed puncture path leading to pneumothorax, severe cardiac, hepatic, pulmonary or renal insufficiency, and unable to tolerate puncture or were unsuitable for the puncture in a supine position.

The experimental miniature pigs were fed in isolation 1 week before puncture in a 12-hour light-dark cycle with normal temperature and humidity. Standard chow and sterile water were available ad libitum. All pigs were fasted 12 hours before the operation. During the puncture operation, the experimental pigs were intramuscularly injected with an anesthetic (Zoletil, 5 mg/kg) and atropine sulfate (0.08 mg/kg). A vein injection needle was placed in the ear marginal vein to establish a vein passage. After tracheal intubation under general anesthesia, pigs were mechanically ventilated by injecting propofol and inhaling isoflurane. Gas anesthesia (isoflurane) was used for animal anesthesia. The intraoperative electrogram was monitored in real-time through limb leads. Intraoperative oxygen saturation was monitored through an oxygen saturation monitor clamped to the pig tongue.

Grouping

In our animal experiments, 30 simulated pulmonary lesions were created in 5 pigs (6 lesions per pig, with 3 per lung) and divided into 2 groups with a 1:1 ratio in a non-randomized manner. Within 1 pig, 3 lesions were punctured with the robot-assisted puncture system and another 3 were performed by the traditional CT-guided manual method. All punctures used a 13.8 cm long 15-gauge disposable coaxial biopsy needle (Bard, Tempe, AZ, USA). At the end of the experiments, the pigs were euthanized using intravenous injections of potassium chloride.

Pulmonary lesion simulation and biopsy specimen definition

First, 10 mL of the non-ionic iodinated contrast agent ioversol was mixed with 10 mL of a 50% aqueous starch mixture to create an ioversol starch mixture. Next, 0.5 mL of the ioversol starch mixture was injected into the bilateral lung tissues of 5 pigs. The average diameter of each injection point was about 1 cm (the simulated lesion). After injection, a chest CT was used to measure the distance between the simulated focus center and chest wall, evaluate the feasibility of establishing the focus model, and confirm that there were no apparent complications, such as pneumothorax and bleeding. The simulated lesions in this experiment had a diameter of 8–16 mm. *Figure 1* shows the simulated lesions in the lung CT images of pigs 1–5.

After the puncture needle arrived at the simulated lesion, the cutting biopsy needle was used for sampling. The tissue was stained with ioversol drop dye to confirm whether the sample successfully contained the simulated lesion. *Figure 2A* shows the ioversol starch mixture after ioversol dripping (blue) as a positive control. *Figure 2B* shows a typical lung tissue specimen as a negative control. A puncture was considered unsuccessful when it comprised normal lung tissue (*Figure 2C*, yellow-red after staining). However, a sample containing a mixture of lung tissue and iodophor starch would be yellow-blue after staining (*Figure 2D*), indicating a successful puncture.

Optical navigation robot-assisted puncture system for percutaneous lung biopsies (PLBs)

An optical navigation robot-assisted puncture system was developed by Shenzhen Wuerzburg Dynamic Inc. It comprised a hardware station, a navigation station, a guide, optical markers, and lung puncture navigation software. The hardware station comprised a touch screen, an optical tracking system, and a high-performance computer for human-computer interaction and optical measurements. The navigation station included a multi-axis robotic arm for automatic puncture. The navigation software was installed on the computer for CT image processing, puncture path planning, and robotic arm control. The guide was combined with the robotic arm to guide the puncture needles. The optical markers were attached to the patient's body surface for lung motion tracking.

The entire percutaneous lung puncture process using this robotic system is illustrated in *Figure 3*, comprising the following 4 steps:

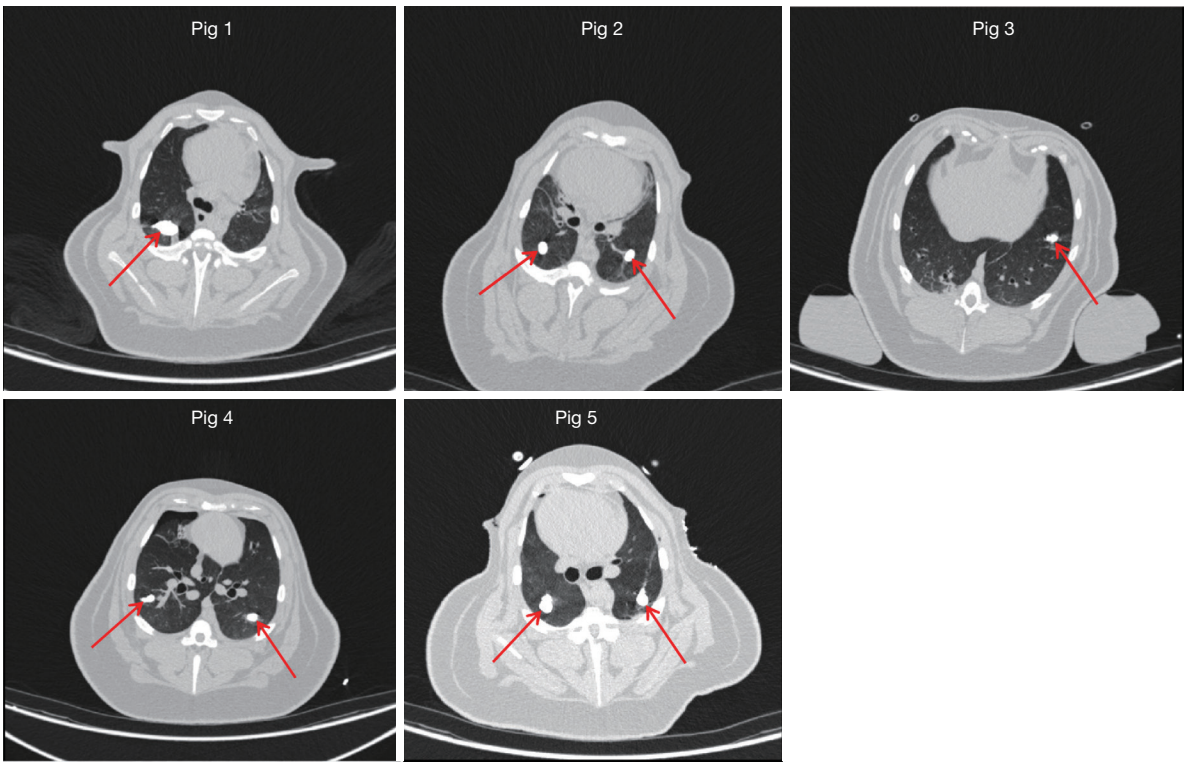

Figure 1 CT images of simulated pulmonary lesions for pigs 1–5, the red arrows indicate the simulated lesions. CT, computed tomography.

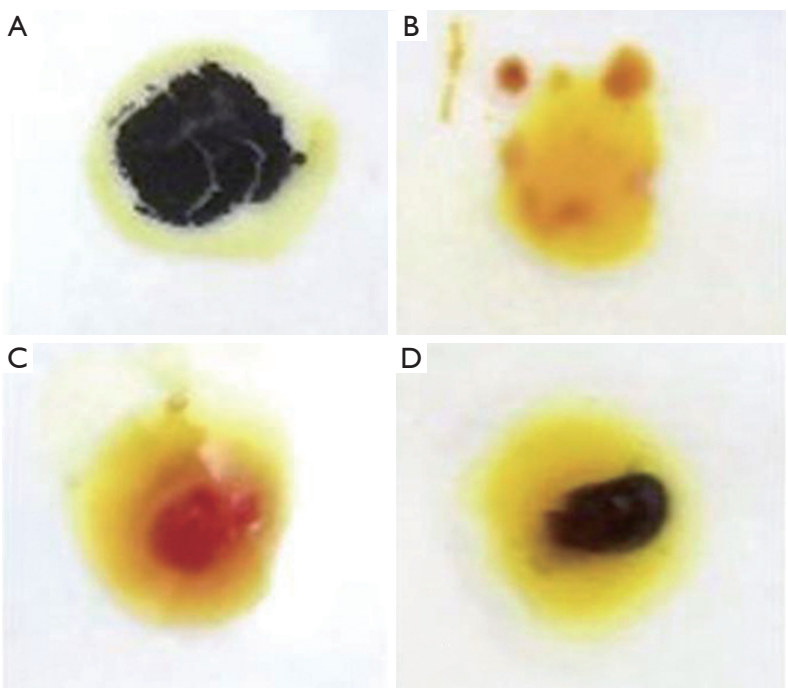

Figure 2 Dyeing contrast. (A) Positive sample. (B) Negative sample. (C) Normal lung tissue. (D) Simulated lesion. Staining method: ioversol drop dye.

- Step 1: system initialization. In this step, the optical markers are fixed on the chest and abdomen of the pig to register and calibrate its breathing status (exhalation and inspiration). Then, CT images of the lung before the puncture are collected and loaded into the navigation software for 3-dimensional (3D) reconstruction of the lung (*Figure 4*).
- Step 2: path planning. The navigation software automatically locates the reference markers in the 3D images. Based on the lung's 3D image, the surgeon plans the needle trajectory in the navigation software to reach the target lesions and avoid bones, essential structures, and organs. The monitor shows the puncture path clearly, and the physician can recheck the path to ensure a safe and unobstructed trajectory (*Figure 5*).
- Step 3: operation navigation. The robotic mechanical arm is connected to a needle guidance device. The operator previews the guide's target position on the monitor to control the robotic arm's movement. The animal's position information obtained through the optical tracking system is registered in real-time with the 3D model to plan the puncture path in the navigation software and virtually reconstruct the path. Then, the robotic arm guides the needle-feeding guide device to the predetermined path with a proper orientation toward the planned puncture trajectory.
- Step 4: puncture. After disinfecting the skin at the puncture site, the puncture needle is sent through the needle guide device according to the needle

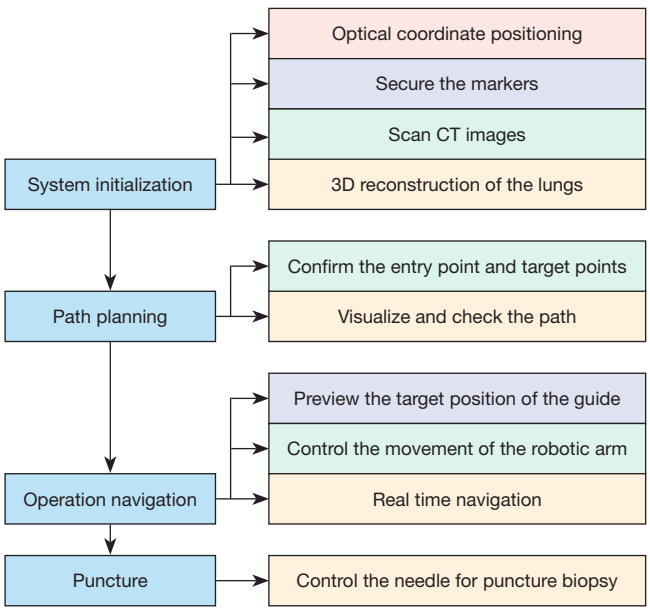

Figure 3 Flowchart of the navigation and positioning system process for percutaneous lung biopsy. CT, computed tomography; 3D, 3-dimensional.

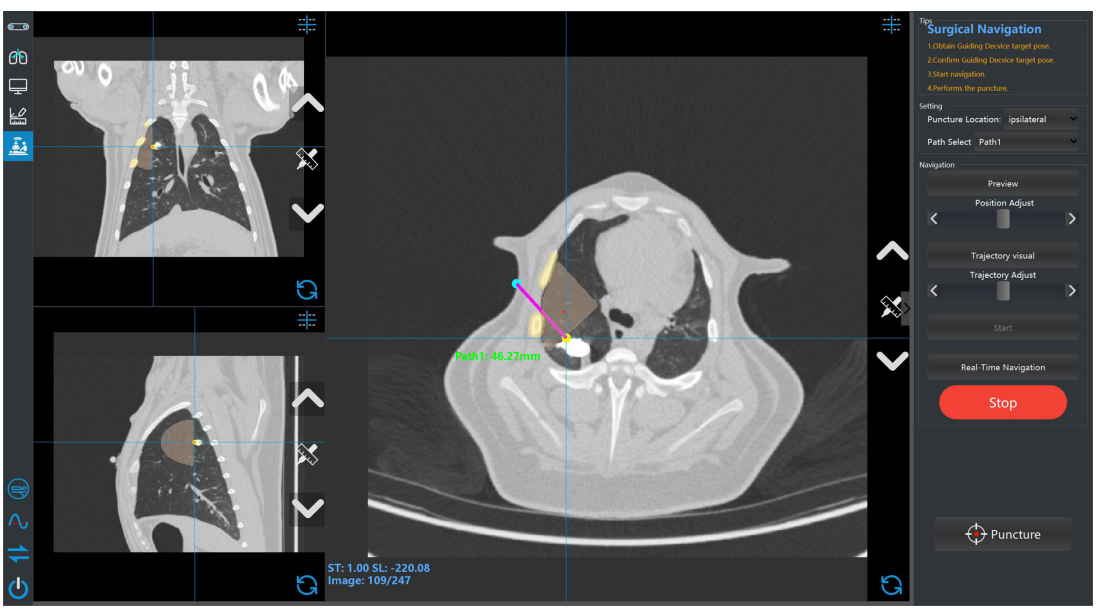

Figure 4 A CT scan of a simulated pulmonary lesion. CT, computed tomography.

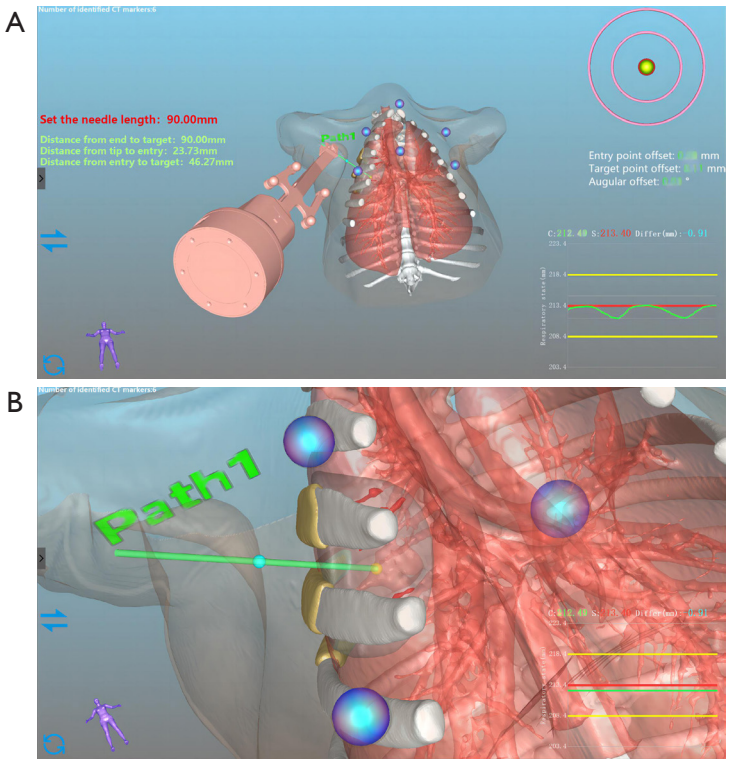

Figure 5 Lung 3D reconstruction and puncture path planning. (A) Overall view. (B) Partial view. 3D, 3-dimensional.

Figure 6 An operator uses this robot-assisted puncture system for biopsy in an experimental pig.

depth calculated by the navigation software. Next, the guide slot's clamping knob is adjusted to separate it from the puncture needle. Then, a recheck pulmonary CT scan is performed to confirm the puncture needle's position (*Figure 6*).

Traditional CT-guided PLB

In the traditional manual CT-guided percutaneous puncture procedure, an experienced operator determines the needle insertion trajectory based on the initial CT image. The entry point is determined using the CT scan frame laser line to indicate the axial position. Since the operator chooses the needle angle based on their experience, they must repeatedly adjust the needle's direction and depth based on multiple CT scans to ensure a safe and accurate puncture.

Evaluation metrics

In our experiment, several metrics were calculated to evaluate the puncture accuracy and safety of the conventional CT-guided manual method and the optical navigation puncture robot-assisted system. The puncture accuracy was evaluated by comparing the preoperative plan

Table 1 Pre-experiment results for operations assisted by the navigation system

Location	Nodule	First needle tip to target point deviation (mm)	Operation time (min)	Success with a single puncture	Number of adjustments	Biopsy result	Puncture complication	Biopsy complication
Pig Pre. 1								
RL	1	1.5	7	P	0	P	–	–
	2	1.4	8	P	0	P	–	Bleeding
	3	0.5	5	P	0	P	–	Bleeding
LL	4	5.3	5	P	0	P	–	–
	5	2.8	8	P	0	P	–	–
Pig Pre. 2								
RL	1	1.5	8	P	0	P	–	Subcutaneous emphysema
	2	2.5	6	P	0	N	–	Bleeding
	3	4.7	9	P	0	P	–	Bleeding
	4	2.5	5	P	0	P	–	Pneumothorax
	5	2.5	4	P	0	P	–	–
LL	6	NA	NA	NA	NA	NA	NA	NA

Pig Pre. 1: the first pig in the pre-experiment; Pig Pre. 2: the second pig in the pre-experiment. RL, right lung; P, positive; LL, left lung; N, negative; NA, not applicable.

with the post-actual puncture point. The Euclidean distance between the simulated lesion's center and the needle's tip and the angle deviation between the actual and planned needle trajectories were measured. The single puncture success rate, needle adjustment times, and biopsy success rate were also calculated. Regarding puncture safety, we focused on 2 complications (pneumothorax and bleeding) during the puncture and biopsy procedures and the operation time. For statistical analysis, continuous variables were expressed as medians (percentile: 25th, 75th) and were compared using the non-parametric Mann-Whitney *U* test.

Results

We first conducted pre-experiments with 2 pigs to perform initial tests of this robot-assisted system. Therefore, the physicians were more familiar with the robotic system and puncture procedure after the pre-experiments. The specific results are shown in *Table 1*.

In the formal experiments, 30 lesions were created (6 lesions per pig, with 3 per lung). The simulated lesions had 6–16 mm diameters, with an average of 10 mm. There were no complications in the lesion modeling process. Both lesion modeling and biopsy operations were performed by the same surgeon. There were no exclusions, and all the 30 lesions were successfully punctured in the robotic group and manual group. No pneumothorax occurred during the localization of all nodules. The puncture paths planned by the physician with the aid of the robotic system accurately avoided blood vessels, and no obvious bleeding complications occurred. The whole robot-assisted puncture process was accurate, safe, and effective. The detailed results for both groups are shown in *Table 2*. The occurrence of complications for both groups are shown in *Table 3*. No technical dysfunction of the navigation system was reported.

Overall, the single puncture success rate was higher in the robot-assisted group (13/15; 86.7%) than in the traditional CT-guided manual group (8/15; 53.3%). The first puncture was closer to the edge of the lesion (1.8±1.7 mm), and the operation time was shorter (7.1±3.7 minutes) in the robot-assisted group than in the manual group (4.4±2.8 mm and 12.9±7.6 minutes, respectively). In the robot-assisted group, the total number of punctures for 15 nodules was 17, and the total number of additional needle adjustments was 2. In the manual group, the total number of punctures for 15 nodules was 31, and the total number of additional needle adjustments was 16. The average number of additional injections was 0.1 in the robot-assisted group and 1.1 in the

Table 2 Experimental percutaneous lung biopsy results

Location	Nodule	Method	First needle tip to lesion distance (mm)	Planning time (min)	Operation time (min)	Success with a single puncture	Number of adjustments	Number of CT scans	Biopsy result	Angle deviation (°)
Pig 1 (m)										
RL	1	R	0	3	5	P	0	3	P	2.5
	2	M	9.0	5	19	N	4	7	P	18.9
	3	M	1.1	2	3	P	0	3	P	4.0
LL	4	R	3.0	5	8	P	0	3	P	6.7
	5	R	5.5	6	6	P	0	3	P	10.2
	6	M	4.1	13	17	N	1	4	P	7.7
Pig 2 (f)										
RL	1	R	1.5	3	6	P	0	3	P	0.6
	2	R	0.4	6	5	P	0	3	P	3.8
	3	M	12.0	8	27	N	4	7	P	11.1
LL	4	R	0.4	5	7	P	0	3	P	0.5
	5	M	2.0	6	27	N	2	5	P	9.5
	6	M	4.0	10	7	P	0	3	P	6.4
Pig 3 (f)										
RL	1	R	2.5	4	15	N	1	4	N	15.0
	2	R	1.0	2	3	P	0	3	P	3.0
	3	M	2.9	7	16	N	2	5	P	15.0
LL	4	R	2.5	2	15	N	1	4	P	16.0
	5	M	4.5	8	12	P	0	3	N	12.0
	6	M	4.1	5	9	N	1	4	P	9.0
Pig 4 (f)										
RL	1	M	5.1	4	5	P	0	3	P	5.0
	2	M	4.9	4	5	P	0	3	P	5.0
	3	M	4.0	17	21	N	2	5	P	21.0
LL	4	R	0	3	6	P	0	3	P	6.0
	5	R	1.1	4	4	P	0	3	P	4.0
	6	R	0	3	5	P	0	3	P	5.0
Pig 5 (f)										
RL	1	R	5.4	9	12	P	0	3	P	12.0
	2	R	2.0	4	5	P	0	3	P	5.0
	3	R	1.5	2	4	P	0	3	P	4.0
LL	4	M	2.9	7	8	P	0	3	P	8.0
	5	M	0.9	5	6	P	0	3	P	6.0
	6	M	3.9	9	12	P	0	3	P	12.0

CT, computed tomography; m, male; RL, right lung; R, optical navigation puncture robotic system; P, positive; M, conventional CT-guided manual method; N, negative; LL, left lung; f, female.

Table 3 Percutaneous lung biopsy complications

Location	Nodule	Method	Puncture complication		Biopsy complication	
			Bleeding	Pneumothorax	Bleeding	Pneumothorax
Pig 1						
RL	1	R	–	–	–	–
	2	M	–	–	–	–
	3	M	–	–	+	+
LL	4	R	–	–	–	–
	5	R	–	–	+	–
	6	M	–	–	–	–
Pig 2						
RL	1	R	–	–	–	–
	2	R	–	–	–	–
	3	M	–	–	–	–
LL	4	R	–	–	–	–
	5	M	–	–	–	–
	6	M	–	–	+	–
Pig 3						
RL	1	R	–	–	–	–
	2	R	–	–	–	–
	3	M	–	–	–	–
LL	4	R	–	–	–	–
	5	M	–	–	–	–
	6	M	–	–	–	–
Pig 4						
RL	1	M	–	–	+	–
	2	M	–	–	+	–
	3	M	–	–	+	–
LL	4	R	–	–	–	–
	5	R	–	–	+	–
	6	R	–	–	+	–
Pig 5						
RL	1	R	–	–	–	–
	2	R	–	–	+	–
	3	R	–	–	–	–
LL	4	M	–	–	–	–
	5	M	–	–	+	–
	6	M	–	–	–	–

–, without complication; +, with complication. RL, right lung; R, optical navigation puncture robotic system; M, conventional CT-guided manual method; CT, computed tomography; LL, left lung.

manual group. There were significant differences between the robot-assisted group and the manual group in single puncture success rate (86.7% *vs.* 53.3%, respectively), first needle tip to target point deviation (P=0.006), total operation time (P=0.007), and the number of needle adjustments (P=0.029). When multiple biopsies (≤3) were allowed, the positive biopsy success rate was 93.3% in both groups. The primary complication in both groups was slight bleeding, with an incidence of 26.7% in the robot-assisted group and 40% in the manual group. There was 1 pneumothorax case in the manual group. No deaths occurred in either group.

Discussion

Our animal experimental results show that performing lung biopsies in a pig lung nodule model using an optical navigation robot-assisted puncture system is accurate and safe. The needle insertion assisted by this robotic system showed higher single puncture accuracy than the manual needle insertion method, with fewer needle adjustments and reduced operation time. Moreover, bleeding complications were lower in the robot-assisted group than in the manual group. Since the robot-assisted system reduces needle insertion adjustments due to wrong direction and depth, puncture time is shortened, decreasing the risks of pneumothorax, bleeding, and radiation exposure. Before the puncture, we planned the puncture path based on the lung lesion, selected the shortest puncture distance, avoided cross-lobar fissure punctures, used coaxial puncture needles, and reduced the number of punctures. These measures also reduced the incidence of pneumothorax and hemorrhage.

The optical navigation robot-assisted system is a new puncture system combining a near-infrared optical navigation function with a multi-degree-of-freedom robotic arm. The robotic system uses the preoperative CT image to reconstruct the relationship between the target lesion and its surrounding vessels, airways, and bones for puncture path planning. Therefore, it can provide detailed 3D spatial information for an accurate and safe puncture (*Figure 5*). Visual puncture path planning in this robotic system maximizes puncture safety. The robotic arm improves the accuracy and stability of precise needle insertion during puncture and reduces needle entry angle and depth errors caused by human limitations. Therefore, the robotic system can achieve highly accurate target positioning in real-time and improve puncture accuracy. The success rate of single needle placement assisted by this robotic system was 86.7% in this animal study.

With advances in image processing technologies and deep learning algorithms, the robot-assisted puncture system makes the puncture process more visual, intelligent, and simple (15). Compared to the traditional CT-guided manual method, the robot-assisted puncture system has the advantages of higher accuracy, shorter operation time, and no increase in radiation exposure (16,17). The operator's technology and experience influence CT-guided PLB. Interventional physicians should be familiar with the lesion's anatomical structure and surrounding tissues and have in-depth imaging knowledge (18). Although several devices and robots have been evaluated to assist out-of-plane needle insertion, only commercial optical and electromagnetic systems are widely used in clinical practice (19-22).

Grasso *et al.* (22) described a clinical test similar to ours. In a non-randomized study of 180 patients, lung biopsies with an optical tracking navigation system (SIRIO; Masmec Biomedical Division, Modugno, Bari, Italy) significantly reduced operation times, control scanning times, and radiation doses. Another study showed that this SIRIO optical navigation system was more accurate for PLB with lesions <20 mm (21). It could also be used to guide the biopsy of pulmonary ground glass lesions with a lower incidence of post-procedural complications, a significant reduction in the radiation dose administered to patients, and a higher diagnostic success rate (23).

The primary disadvantage of these optical systems is that the camera and optical markers cannot be obstructed. Although electromagnetic navigation systems are not limited by light blocking, their performance can be affected by metal or other magnetic disturbances (24). A retrospective study by Lanouzière *et al.* assessed the efficacy of a CT-navigation electromagnetic system compared to the conventional CT method for PLBs (25). The diagnostic success rate was similar in both groups. There was no significant difference in total operation time, the total number of CT acquisitions, and complication rate. This electromagnetic navigation system was effective and safe compared to the traditional CT method for PLBs. Another study showed that an electromagnetic navigation system could improve puncture accuracy, reduce distance error, and reduce the number of CT scans. The navigation system (Imactis SAS; La Tronche, Auvergne-Rhône-Alpes, France) was accurate under clinical conditions, even with occasional and non-expert surgeons (20). However, the electromagnetic navigation system's magnetic field was easily interfered.

Technical failures may occur, especially in the CT environment. One previous study showed that 8 of 26 patients needing electromagnetic navigation had technical shortcomings (26). Unlike rigid and static organs such as the brain and bone, robot-assisted puncture systems might experience errors in lung puncture (27). Since respiratory movement changes the target point of lung lesions, preoperative image data cannot be aligned in real-time with patients' pulmonary anatomy data, making the widespread use of navigation technology in lung puncture challenging.

The optical tracking system could track the optical marker in real time and guide the needle insertion orientation and depth. The robotic arm controls the puncture trajectory to reduce errors caused by manual operation. This novel system can guide the non-coplanar puncture and optimize the puncture path for those lesions with bones and blood vessels obstructing the coplanar puncture path. In our study, the needle insertion assisted by this optical navigation puncture robotic system had a higher single puncture success rate than manual needle insertion, with fewer needle adjustments and confirmatory CT scans needed. Moreover, radiation exposure was lower in the robot-assisted group than in the CT-guided manual puncture group.

CT-guided PLB has been shown to be a safe and feasible diagnostic method. However, the accuracy and safety of PLB are greatly influenced by the proficiency of the operator. In this study, robot-assisted puncture systems, experienced surgeons, and beginners were not compared. However, the robot-assisted system can provide specific guidance for young doctors without any experience in puncture biopsy, providing beginners with more experience and confidence. Experienced surgeons and puncture navigation robots both have their unique advantages and are not in conflict. We will continue to conduct relevant research to explore deeper integration and assistance between them, in order to achieve better medical outcomes.

However, our study had some limitations. First, it was a single-center, non-randomized animal experiment with only 5 pigs and 30 simulated lesions. The simulated lesions' location and size in the experimental animals were limited. The puncture needle types used in this study were limited. Second, the simulated nodules used in this study were not actual tumors. Finally, the breath-holding technology of the ventilator used in the animal experiment differs from that for conscious patients.

Conclusions

Overall, our optical navigation robot-assisted puncture system is a novel device combining near-infrared optical positioning technology and robotic arm control. Robot-assisted needle insertion in the lung nodule using this device was tested in a pig model. The results show that it is feasible, safe, and accurate for PLB. Compared to the traditional CT-guided manual puncture, this robot-assisted puncture system increased the single puncture success rate. It also reduced the number of CT scans, radiation dose, and needle manipulation times and had equivalent accuracy to conventional CT-guided biopsy. Based on the successful outcomes of this animal experiment, this system's effectiveness and feasibility in human patients will be evaluated in subsequent clinical trials.

Acknowledgments

Funding: This study was supported by the Major Science and Technology Special Plan of Biological Medicine of Yunnan Province (No. 0202002AA100075 to Jing Li), the Project of the Educational Commission of Guangdong Province of China (No. 2022ZDJS113 to Bingding Huang), and the School-Enterprise Cooperation Fund provided by Wuerzburg Dynamics Inc. to the Weiding Joint Laboratory of Medical Artificial Intelligence, Shenzhen Technology University (to Bingding Huang).

Footnote

Reporting Checklist: The authors have completed the ARRIVE reporting checklist. Available at https://qims.amegroups.com/article/view/10.21037/qims-23-576/rc

Conflicts of Interest: All authors have completed the ICMJE uniform disclosure form (available at https://qims.amegroups.com/article/view/10.21037/qims-23-576/coif). Jing Li reports that this research was funded by the Major Science and Technology Special Plan of Biological Medicine of Yunnan Province (No. 0202002AA100075). BH reports that this research was funded by the Project of the Educational Commission of Guangdong Province of China (No. 2022ZDJS113) and the School-Enterprise Cooperation Fund provided by Wuerzburg Dynamics Inc. to Shenzhen Technology University. Jun Liu is an employee of Wuerzburg Dynamics Inc., Shenzhen. WX is the founder

of Wuerzburg Dynamics Inc., Shenzhen. The other authors have no conflicts of interest to declare.

Ethical Statement: The authors are accountable for all aspects of the work in ensuring that questions related to the accuracy or integrity of any part of the work are appropriately investigated and resolved. All animal experiments were performed in compliance with institutional guidelines for the care and use of animals and the study protocol was approved by the Ethics Committee of Guangdong Provincial People's Hospital (No. KV-Q-2022-214-01).

References

1. Siegel RL, Miller KD, Fuchs HE, Jemal A. Cancer statistics, 2022. CA Cancer J Clin 2022;72:7-33.
2. Wood DE, Kazerooni EA, Aberle D, Berman A, Brown LM, Eapen GA, et al. NCCN Guidelines® Insights: Lung Cancer Screening, Version 1.2022. J Natl Compr Canc Netw 2022;20:754-64.
3. Schreiber G, McCrory DC. Performance characteristics of different modalities for diagnosis of suspected lung cancer: summary of published evidence. Chest 2003;123:115S-28S.
4. Liu Y, Wang F, Zhang Q, Tong Z. Diagnostic yield of virtual bronchoscope navigation combined with radial endobronchial ultrasound guided transbronchial cryo-biopsy for peripheral pulmonary nodules: a prospective, randomized, controlled trial. Ann Transl Med 2022;10:443.
5. Asano F, Ishida T, Shinagawa N, Sukoh N, Anzai M, Kanazawa K, Tsuzuku A, Morita S. Virtual bronchoscopic navigation without X-ray fluoroscopy to diagnose peripheral pulmonary lesions: a randomized trial. BMC Pulm Med 2017;17:184.
6. Ali MS, Trick W, Mba BI, Mohananey D, Sethi J, Musani AI. Radial endobronchial ultrasound for the diagnosis of peripheral pulmonary lesions: A systematic review and meta-analysis. Respirology 2017;22:443-53.
7. Nadig TR, Thomas N, Nietert PJ, Lozier J, Tanner NT, Wang Memoli JS, Pastis NJ, Silvestri GA. Guided Bronchoscopy for the Evaluation of Pulmonary Lesions: An Updated Meta-analysis. Chest 2023;163:1589-98.
8. Manhire A, Charig M, Clelland C, Gleeson F, Miller R, Moss H, Pointon K, Richardson C, Sawicka E; BTS. Guidelines for radiologically guided lung biopsy. Thorax 2003;58:920-36.
9. Kiranantawat N, McDermott S, Fintelmann FJ, Montesi SB, Price MC, Digumarthy SR, Sharma A. Clinical role, safety and diagnostic accuracy of percutaneous transthoracic needle biopsy in the evaluation of pulmonary consolidation. Respir Res 2019;20:23.
10. Zhou Q, Dong J, He J, Liu D, Tian DH, Gao S, et al. The Society for Translational Medicine: indications and methods of percutaneous transthoracic needle biopsy for diagnosis of lung cancer. J Thorac Dis 2018;10:5538-44.
11. Wiener RS, Schwartz LM, Woloshin S, Welch HG. Population-based risk for complications after transthoracic needle lung biopsy of a pulmonary nodule: an analysis of discharge records. Ann Intern Med 2011;155:137-44.
12. Zhao Y, Mei Z, Luo X, Mao J, Zhao Q, Liu G, Wu D. Remote vascular interventional surgery robotics: a literature review. Quant Imaging Med Surg 2022;12:2552-74.
13. Dong J, Zhang L, Li W, Mao S, Wang Y, Wang D, Shen L, Dong A, Wu P. 1.0 T open-configuration magnetic resonance-guided microwave ablation of pig livers in real time. Sci Rep 2015;5:13551.
14. Li ZC, Li K, Zhan HL, Chen K, Chen MM, Xie YQ, Wang L. Augmenting interventional ultrasound using statistical shape model for guiding percutaneous nephrolithotomy: Initial evaluation in pigs. Neurocomputing 2014;144:58-69.
15. Unger M, Berger J, Melzer A. Robot-Assisted Image-Guided Interventions. Front Robot AI 2021;8:664622.
16. Smakic A, Rathmann N, Kostrzewa M, Schönberg SO, Weiß C, Diehl SJ. Performance of a Robotic Assistance Device in Computed Tomography-Guided Percutaneous Diagnostic and Therapeutic Procedures. Cardiovasc Intervent Radiol 2018;41:639-44.
17. Cornelis F, Takaki H, Laskhmanan M, Durack JC, Erinjeri JP, Getrajdman GI, Maybody M, Sofocleous CT, Solomon SB, Srimathveeravalli G. Comparison of CT Fluoroscopy-Guided Manual and CT-Guided Robotic Positioning System for In Vivo Needle Placements in Swine Liver. Cardiovasc Intervent Radiol 2015;38:1252-60.
18. Yoon SH, Lee SM, Park CH, Lee JH, Kim H, Chae KJ,

Jin KN, Lee KH, Kim JI, Hong JH, Hwang EJ, Kim H, Suh YJ, Park S, Park YS, Kim DW, Choi M, Park CM. 2020 Clinical Practice Guideline for Percutaneous Transthoracic Needle Biopsy of Pulmonary Lesions: A Consensus Statement and Recommendations of the Korean Society of Thoracic Radiology. Korean J Radiol 2021;22:263-80.
19. Zhang Y, Huang H, Cao S, Teng J, Wang Y, Ling X, Zhou Y, Xu J, Li W, Zhong H. Clinical value of an electromagnetic navigation system for CT-guided percutaneous lung biopsy of peripheral lung lesions. J Thorac Dis 2021;13:4885-93.
20. Durand P, Moreau-Gaudry A, Silvent AS, Frandon J, Chipon E, Médici M, Bricault I. Computer assisted electromagnetic navigation improves accuracy in computed tomography guided interventions: A prospective randomized clinical trial. PLoS One 2017;12:e0173751.
21. Grasso RF, Faiella E, Luppi G, Schena E, Giurazza F, Del Vescovo R, D'Agostino F, Cazzato RL, Beomonte Zobel B. Percutaneous lung biopsy: comparison between an augmented reality CT navigation system and standard CT-guided technique. Int J Comput Assist Radiol Surg 2013;8:837-48.
22. Grasso RF, Luppi G, Cazzato RL, Faiella E, D'Agostino F, Beomonte Zobel D, De Lena M. Percutaneous computed tomography-guided lung biopsies: preliminary results using an augmented reality navigation system. Tumori 2012;98:775-82.
23. Faiella E, Messina L, Castiello G, Bernetti C, Pacella G, Altomare C, Andresciani F, Sarli M, Longo F, Crucitti P, Beomonte Zobel B, Grasso RF. Augmented reality 3D navigation system for percutaneous CT-guided pulmonary ground-glass opacity biopsies: a comparison with the standard CT-guided technique. J Thorac Dis 2022;14:247-56.
24. Sorriento A, Porfido MB, Mazzoleni S, Calvosa G, Tenucci M, Ciuti G, Dario P. Optical and Electromagnetic Tracking Systems for Biomedical Applications: A Critical Review on Potentialities and Limitations. IEEE Rev Biomed Eng 2020;13:212-32.
25. Lanouzière M, Varbédian O, Chevallier O, Griviau L, Guillen K, Popoff R, Aho-Glélé SL, Loffroy R. Computed Tomography-Navigation™ Electromagnetic System Compared to Conventional Computed Tomography Guidance for Percutaneous Lung Biopsy: A Single-Center Experience. Diagnostics (Basel) 2021;11:1532.
26. Grand DJ, Atalay MA, Cronan JJ, Mayo-Smith WW, Dupuy DE. CT-guided percutaneous lung biopsy: comparison of conventional CT fluoroscopy to CT fluoroscopy with electromagnetic navigation system in 60 consecutive patients. Eur J Radiol 2011;79:e133-6.
27. Kim D, Han JY, Baek JW, Lee HY, Cho HJ, Heo YJ, Shin GW. Effect of the respiratory motion of pulmonary nodules on CT-guided percutaneous transthoracic needle biopsy. Acta Radiol 2023;64:2245-52.

Cite this article as: Li J, Su L, Liu J, Peng Q, Xu R, Cui W, Deng Y, Xie W, Huang B, Chen J. Optical navigation robot-assisted puncture system for accurate lung nodule biopsy: an animal study. Quant Imaging Med Surg 2023;13(12):7789-7801. doi: 10.21037/qims-23-576

